

# Ballistic properties of debris produced by laser shock-induced micro-spallation of tin samples

**D Loison, T de Resseguier and A Dragon**

Institut P<sup>7</sup> – CNRS UPR 3346 – Département Physique Mécanique des Matériaux  
1 avenue Clément Ader BP 40109  
F86961 FUTUROSCOPE CHASSENEUIL, FRANCE

E-mail: didier.loison@ensma.fr

**Abstract.** Dynamic fragmentation in the liquid state after melting under shock compression or upon release leads to the ejection of a cloud of droplets. This phenomenon, called micro-spallation, remains essentially unexplored in most metals. We present laser shock experiments performed on tin, to pressures ranging from about 60 to 220 GPa. Experimental diagnostics include skew Photonic Doppler Velocimetry (PDV) measurements of the droplets velocities, transverse observations of the expanding cloud of droplets, and soft recovery of ejecta within a low density gel. Optical microscopy of the gel reveals the presence of droplets which confirm shock-induced melting prior to fragmentation. To quantify size distribution of the debris, 3D X-ray micro-tomography has been performed at the ESRF synchrotron facility in France (similar to US Advanced Photon Source), where sub-micrometer resolution could be achieved. In this paper, the resulting velocity and size distributions are presented and compared with theoretical predictions based on a one-dimensional description accounting for laser shock loading, wave propagation, phase transformations, and fragmentation. Discrepancies between measured and calculated distributions are discussed. Finally, combining size and velocity data provides estimates of the ballistic properties of debris and their kinetic energy, which are key issues for anticipating the damage produced by their impacts on nearby equipments.

## 1. Introduction

The generation of high velocity metallic liquid fragments produced by micro-spalling [1] in laser driven shock experiments such as Inertial Confinement Fusion (ICF) can damage vacuum chambers or measurement devices. To assess and reduce such risks of damage, the fragment size and ejection velocity must be efficiently predicted by models based on experimental data. So, physics of the creation, dispersion and re-collection of the cloud of droplets on a distant obstacle require both theoretical and experimental research work.

In this context, we have conducted experimental investigations of melting and micro-spalling in tin and aluminium under laser driven shocks. Experimental diagnostics include Photonic Doppler Velocimetry (PDV) measurements to probe velocity distribution in the expanding cloud [2], transverse optical shadowgraphy and soft recovery of the ejecta in low density gel [3] for post-shock observations by optical microscopy or micro-tomography. These techniques provide complementary results which allow determining size and velocity distributions of debris ejected by micro-spallation



useful for the development and validation of models. In this paper, we focus on the ballistic properties of debris produced by laser shock induced micro-spallation of tin samples.

## 2. Experimental procedure

Laser shots have been performed in the Laboratoire pour l'Utilisation des Lasers Intenses (LULI, UMR 7605, Ecole Polytechnique, Palaiseau, France) on the “nano2000” facility. The samples are 50  $\mu\text{m}$ -thick tin foils of 99.99% purity. A high power pulsed laser beam of 1.06  $\mu\text{m}$  wavelength, 3 ns duration, and 1400 J maximum energy is focused onto the target. The irradiated spot is circular with a diameter of 2–3 mm. The setup is placed in a vacuum chamber to avoid laser breakdown in air before reaching the target surface. The laser irradiation produces the vaporization of a thin layer of material, transformed into a plasma cloud, whose expansion toward the laser source induces by reaction a compressive pulse into the solid target.

A PDV system developed and kindly provided by the CEA Bruyères-le-Chatel, France [2] allows time-resolved measurement of the velocity of the debris ejected from the free surface, opposite to the loaded surface. To obtain velocity distribution throughout the expanding debris cloud, the PDV probe is placed at a 15° tilt angle from the normal to the free surface [4]. Transverse shadowgraphy fully described elsewhere [3] provides successive images of the expanding cloud, which allow estimate the mean velocity of the fastest debris. A soft recovery device is used to collect the droplets. It is composed of a low density gel (0.9) which limits secondary fragmentation or recombination of the fragments. After each shot, the gel can be studied in optical microscopy and/or X-ray micro-tomography.

## 3. Models

The amplitude of the pressure load and its temporal shape are inferred from one-dimensional computations of laser-matter interaction, using the measured profile of laser intensity as input for the Lagrangian code ESTHER. Subsequent propagation and interactions of compression and release waves within the sample are simulated with the hydrocode SHYLAC where multi phase equations of state and fragmentation models have been implemented. Each phase is modeled by an equation of state based on Birch isotherm which expresses pressure  $p$  as a function of specific volume  $v$  and temperature  $T$  [5]. To model the kinetics of phase transitions, we used the Hayes formulation [6, 7] to calculate mass proportion as a function of Gibbs free enthalpy gap between phases and characteristic time of each phase transition. Finally, an energetic approach proposed by Grady is used to model fragmentation in the liquid state with a horizon condition to predict the debris size [8, 9, 10].

## 4. Results and discussion

Figure 1 presents a PDV record of the velocity distribution behind a 50  $\mu\text{m}$ -thick tin foil subjected to a 160 GPa laser shock. The measurement (dots) is compared to the simulated profiles (lines). Thin solid lines account for the spreading of the theoretical profile due to the finite diameter of the PDV probe beam.

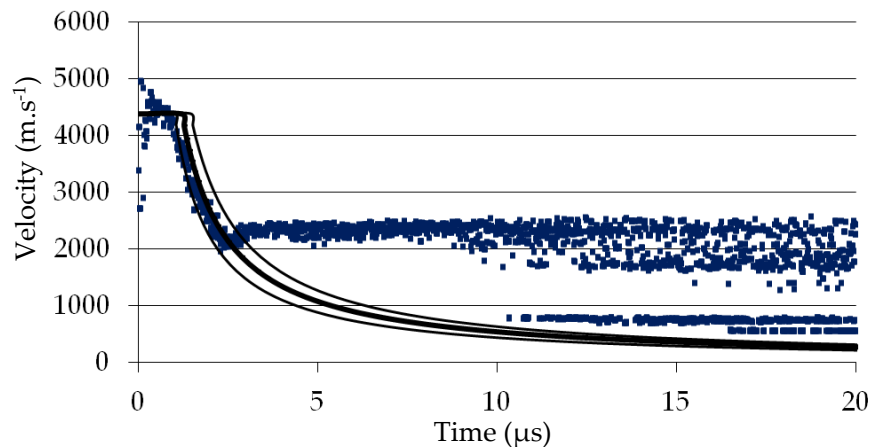


**Figure 1:** Comparison of measured (dots) and simulated (solid lines) velocity profiles in the micro-spall expanding from a 50  $\mu\text{m}$ -thick tin sample subjected to a 160 GPa laser shock.

Highest ejection velocities are about 4500 m/s. They correspond to velocities of droplets constituting the front of the cloud which mask the following droplets for the first two microseconds. After the plateau, this main front is no longer intercepted by the PDV probe, set at a  $15^\circ$  tilt angle from the expansion direction, but slower particles are detected, so that both measured and theoretical velocity curves drop with a marked upward concavity. A correct consistency is found between measured and theoretical profiles for the first few  $\mu\text{s}$ . The evolution of the fragments velocity within the debris cloud is continuous and monotonous. After a few  $\mu\text{s}$ , the measured profile exhibits a clear, approximately constant velocity trace which seems to superimpose on the decreasing velocity curve consistent with the 1D theoretical approach. This trace is attributed to the late ejection of secondary fragments from the edges of the loaded zone due to the punching of the target, with centrifugal velocity components. Because some fragments fly along the probe direction, their velocity is measured over long times, but after some time, they do not screen completely the slower part of the micro-spall behind them, which is detected again after  $\sim 10 \mu\text{s}$ . Finally, another 2D effect is the spatial non-uniformity of the pressure load applied on the irradiated spot due to inhomogeneous energy distribution in the laser beam. This results in a non-planar, irregular front of the debris cloud with lower ejection velocities at the periphery of the loaded zone than at its center. This effect, not accounted for in the 1D simulations where the cloud is approximated to have a square shape, explains slight differences between measurements and theory. However, 1D simulation provides a good estimation of the velocity distribution of debris generated by micro-spallation.

To complete ballistic properties of debris, size distributions of fragments have to be determined. Optical micrographs through a gel where tin fragments have been collected reveal a lot of spherical micrometric droplets which confirm micro-spallation in the melted state. To evaluate the number of debris, X-ray micro-tomography of the gels has been performed to reconstruct the three dimensional population of the fragments, using the consistent and high-energy X-ray irradiation available at the ESRF synchrotron facility in France. A first “low resolution” configuration was used to detect all debris larger than  $3.5 \mu\text{m}$ . In a second configuration, the spatial resolution (i.e. size of the voxel) was improved to  $1.4 \mu\text{m}$ , then to  $0.7 \mu\text{m}$ , but the total scanned volume was reduced, with a focus on the deeper zones in the gel (figure 2).

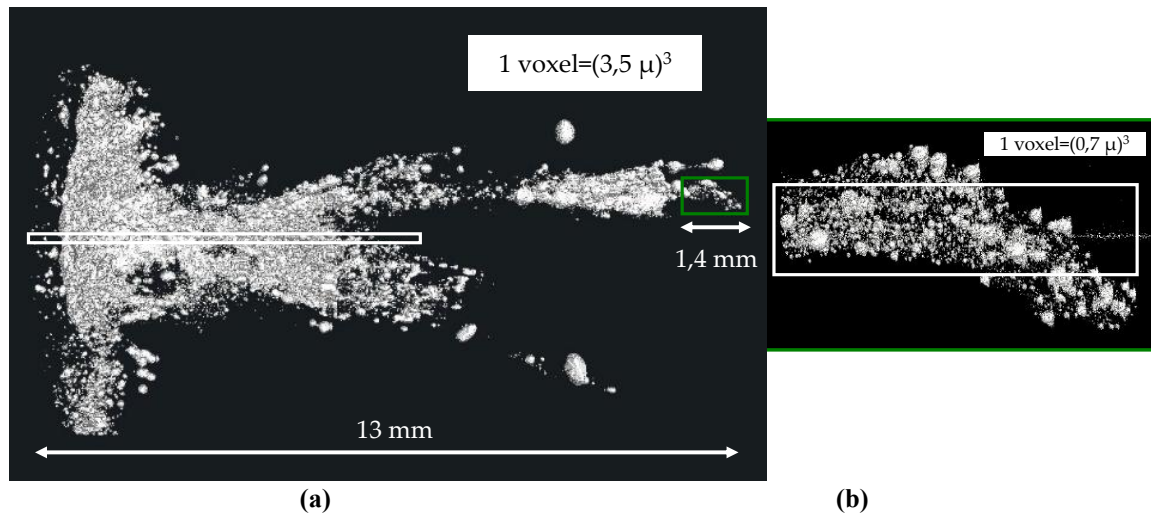


**Figure 2:** 3D reconstruction of the tin fragments recovered in a gel set behind a 50  $\mu\text{m}$  thick sample subjected to a 85 GPa laser pulse. Fragments have penetrated from left to right. Spatial resolution of microtomography is improved from 3.5  $\mu\text{m}$  (a) to 0.7  $\mu\text{m}$  (b) in the small volume inside the green window. White boxes represent volumes selected to compare simulation predictions and experimental results

The *3D object counter* [11] available in the software *Fiji* [12] provides particle size distributions, and penetration depth distribution from 3D reconstruction. By using mass conservation simulated and experimental distributions can be compared (figure 3).

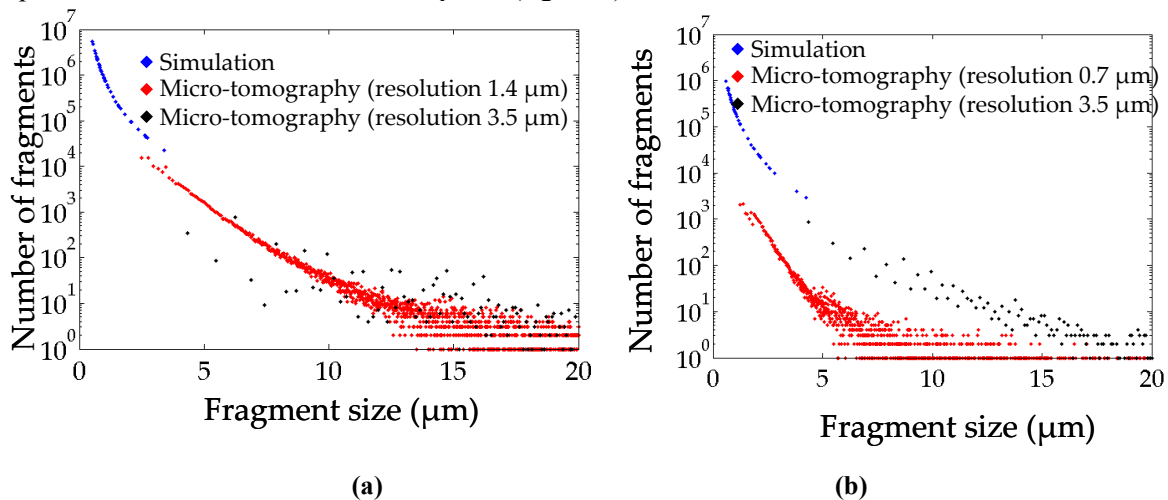


**Figure 3:** Fragment size distributions after a 79 GPa (a) and a 85 GPa (b) laser shock applied onto a 50  $\mu\text{m}$ -thick tin sample. The blue points result from a one-dimensional simulation of the experiment using a global energetic criterion to account for the micro-spall process. The black points show experimental values provided by X ray micro-tomography of the gel. The red points are obtained from high resolution scanning of a small portion of the gel.

In experimental results, the number of large fragments provided by the 3.5  $\mu\text{m}$  resolution micro-tomography is higher than that obtained with the better resolution. This gap has two origins: the first is the difference between the scanned volumes: a cylinder of 14  $\text{mm}^3$  (or 20  $\text{mm}^3$ ) at low resolution against 9  $\text{mm}^3$  (or 2  $\text{mm}^3$ ) at high resolution for the shot of 1.8  $\text{TW}/\text{cm}^2$  (or 3.0  $\text{TW}/\text{cm}^2$ ,

respectively). The second origin is that two very close fragments can be detected as one. This artefact is more important for lower spatial resolution.

The numerical results predict fragment sizes ranging between 0.26  $\mu\text{m}$  and 3.6  $\mu\text{m}$ . This range is consistent with previous studies [13], and with the local micro-tomography with a resolution of 1.4  $\mu\text{m}$  or 0.7  $\mu\text{m}$ . While the simulation predicts the number of fragments produced over the entire thickness of the microspalled target, only a small portion of the gel is scanned at such high resolution, so the number of detected fragments is much lower than the computed one, by a factor 2 for the 1.4  $\mu\text{m}$  resolution and 10 for the 0.7  $\mu\text{m}$  resolution. Besides, tomography detects fragments much larger than predicted. They can arise from the coalescence of smaller droplets when they penetrate into the gel. Indeed, fast drops can open a channel in the gel where slower ones will penetrate more easily, then merge together to form one larger fragment.

To predict potential damage created by these fragments, kinetic energy of ejecta must be calculated. So, we have to associate velocity with particle size (figure 4).

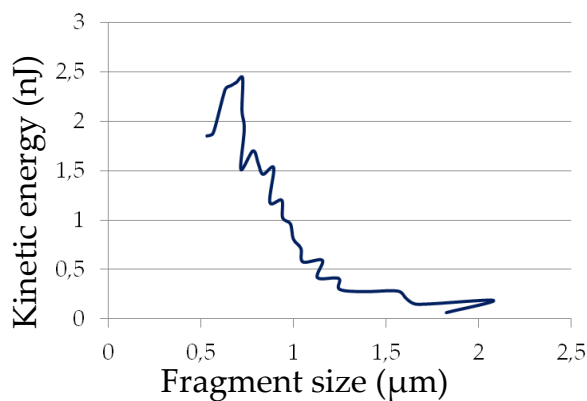


**Figure 4:** Kinetic energy versus size of fragments predicted by simulation after a 79 GPa laser shock applied onto a 50  $\mu\text{m}$ -thick tin sample.

Due to the small mass of the micro-sized fragments, their kinetic energy is very low, of the order of a few nanojoules. This kinetic energy of the fragments decreases rapidly when their size increases. Therefore, the smallest debris are likely to generate the greatest damage. As the penetration of fragments in the gel depends on their kinetic energy, the wide variation of the energy for sizes between 0.5 and 1  $\mu\text{m}$  is consistent with the presence of these fragments everywhere inside the gel. In contrast, larger fragments of size between 1 and 2  $\mu\text{m}$ , have an approximately constant low energy. Because of their size, they should undergo more friction during their penetration. However, smallest and fastest droplets open ways into the gel, and heat it locally, which makes penetration of the following fragments easier. Finally, as discussed above, the gels contain much bigger fragments than these predicted by the simulations. Thus, the experimental depth penetration distribution cannot be related directly to the calculated profile of kinetic energy.

## 5. Conclusion

Dynamic fragmentation of laser shock-melted tin and aluminium has been investigated with complementary diagnostics, including soft recovery and micro tomography of the fragments ejected from the samples. Experimental results are compared to computations involving multiphase equations of state. Ballistic properties of ejected debris are analyzed to predict which fragments are more destructive.

## Acknowledgements

We thank all the staff of the LULI and ESRF for technical support, CEA Bruyères le Chatel for providing the ESTHER code and PDV device, and CEA Valduc for financial support.

## References

- [1] De Resseguier T, Signor L, Dragon A, Boustie M, Roy G and Llorca F 2007 *J. Appl. Phys.* **101** 013506
- [2] Mercier P, Benier J, Azzolina A, Lagrange J M and Partouche D 2006 *J. Phys.* IV **134** 805-12
- [3] Lescoute E, De Resseguier T, Chevalier J M, Boustie M, Cuq-Lelandais J-P and Berthe L 2009 *Appl. Phys. Lett.* **95** 211905
- [4] Loison D, De Resseguier T, Dragon A, Mercier P, Benier J, Deloison G, Lescoute E and Sollier A 2012 *J. Appl. Phys.* **112** (11) 113520.
- [5] Loison D, De Resseguier T, Dragon A, Lescoute E and Boustie M 2011 *AIP Conf. Proc.* **1426** 1545–8
- [6] Hayes D 1975 *J. Appl. Phys.* **46** (8) 3438–43
- [7] Davis J P and Hayes D B 2003 *AIP Conf. Proc.* **706** 163–6
- [8] Grady D 1982 *J. Appl. Phys.* **53** (1) 322–5
- [9] Grady D 1988 *J. Mech. Phys. Solids* **36** (3) 353-84
- [10] Signor L, De Resseguier T, Dragon A, Roy G, Fanget Z and Faessel M 2010 *Int. J. of Impact Engineering* **37** 887-900
- [11] Bolte S and Cordelières F P, *Microscopy J* 2006 **224**, (3), 213-32
- [12] [http://fiji.sc/wiki/index.php/3D\\_Objects\\_Counter](http://fiji.sc/wiki/index.php/3D_Objects_Counter)
- [13] De Rességuiet T, Signor L, Dragon A and Roy G 2010 *Int. J. Fracture* **163** 109-19